NONLINEAR AERODYNAMIC MODELING OF HANSA-3 AIRCRAFT USING NEURAL-GAUSS-NEWTON METHOD

Rakesh Kumar and A.K. Ghosh
Department of Aerospace Engineering
Indian Institute of Technology Kanpur
Kanpur - 208 016, India
Email : rakpec@iitk.ac.in, akg@iitk.ac.in

Abstract

The paper presents the nonlinear longitudinal aerodynamic modeling using Neural-Gauss-Newton (NGN) method from real flight data of Hansa-3 aircraft. The NGN method is an algorithm that utilizes Feed Forward Neural Network and Gauss-Newton optimization to estimate the parameters and it does not require a priori postulation of mathematical model or solution of equations of motion. The Kirchhoff's quasi-steady stall model was used to include the nonlinearity in the aerodynamic model used for parameter estimation. Before application to the flight data at high angles of attack, the method was validated on flight data at moderate angles of attack. The results obtained in terms of stall characteristics and aerodynamic parameters were encouraging and reasonably accurate to establish NGN as a method for modeling nonlinear aerodynamics using flight data at high angles of attack. The supremacy of NGN was established by comparing the NGN estimates to that of Maximum Likelihood.

Nomenclature

a_1 = Static stall characteristics parameter
a_x , a_y , a_z = Horizontal, lateral and vertical component of acceleration, m/s^2
A = Aspect ratio
b = Wing span, m
$\bar{c}$ = Mean aerodynamic chord, m
C_d , C_L , C_m = Drag, lift and pitching moment coefficients
C_{D_0}, C_{L_0}, C_{m_0} = Drag, lift and moment coefficient at zero angle of attack
C_X , C_Y , C_Z = Coefficients of longitudinal, lateral and vertical force
g = Acceleration due to gravity, m/s^2
F_{eng} = Engine thrust, N
I_x , I_y ,I_z = moment of inertia about x,y and z-axis, kg-m^2
I_{xz} = Product of inertial, kg-m^2
J = Cost function
k = General index
m = Aircraft mass, kg
N = Number of data points
p,q,r = Roll, pitch and yaw rates, rad/s
R = Measurement covariance matrix
S = Planform area, m^2
t = Time, s
T = Temperature, ^{o}K
u,v,w = Longitudinal, lateral and vertical airspeed components, m/s
V = Airspeed, m/s
X_o = Steady-state flow separation point
Y = Estimated value
Z = Measured value
α = Angle of attack, rad
α^* = Break point corresponding to X_0=0.5, deg
β = Angle of sideslip, rad
δ_a , δ_e , δ_r = Aileron, elevator and rudder deflection, rad
Δ = Bias, m
φ , θ , ψ = Angles of roll, pitch and yaw and rad
ρ = Density, kg/m^3
σ_{eng} = Angle between flight path and engine thrust line, deg
τ_1 , τ_2 = Time constants representing transient and hysteresis effects, sec

Paper Code : V63 N3/730-2011. Manuscript received on 01 Oct 2010. Reviewed and accepted as a Full Length Contributed Paper on 12 July 2011

Θ, ζ, ξ = Vectors of unknown parameters

Subscripts

ENCG = Distance of engine from center of gravity

Longitudinal Stability and Control Derivatives

$C_{D_\alpha} = \partial C_D / \partial \alpha$, $C_{D_{\delta e}} = \partial C_D / \partial \delta e$, $C_{D_X} = \partial C_D / \partial X$

$C_{L_\alpha} = \partial C_L / \partial \alpha$, $C_{L_q} = \partial C_L / \partial (q\bar{c}/2u)$, $C_{L_{\delta e}} = \partial C_L / \partial \delta e$

$C_{m_\alpha} = \partial C_m / \partial \alpha$, $C_{m_q} = \partial C_m / \partial (q\bar{c}/2u)$, $C_{m_{\delta e}} = \partial C_m / \partial \delta e$

$C_{m_X} = \partial C_m / \partial X$

Introduction

Aircraft parameter estimation [1-10] is probably the most outstanding and illustrated example of system identification methodology. The interest in dynamic behavior of aircraft led to the formulation of the basic equations of motion in the early 20th century. The equations of motion of flight vehicle are derived from Newtonian mechanics. The mathematical models based on such equations of motion assume that the forces and moments acting on the vehicle can be synthesized. Out of the various forces and moments acting on the vehicle, it is the determination of aerodynamic forces that poses the most difficult challenge till date. To a large extent, it is the adequacy and accuracy of modeling of the aerodynamic forces and moments that would determine the validity and utility of the mathematical models. Even today, the flight vehicle identification problems have their main focus on determining the aerodynamic model for high performance and highly augmented unstable aircraft. The model for such a vehicle may have unknown structure or may be highly nonlinear and affected by unsteady aerodynamics associated with stall and erroneous air data measurements. At initial stages of aircraft design, analytical methods provide the only convenient way of estimating the aircraft parameters.

An extensive investigation in the field of unsteady aerodynamics associated with aerodynamic stall at high angles of attack using computational fluid dynamic methods, wind tunnel tests and semi-empirical methods is going on in the recent times. Such models are used to investigate complex flow phenomena analytically, but presenting them in an analytical form suitable for parameter estimation is a difficult task. An alternative approach analytically describes [11-12] the flow separation including stall hysteresis as a function of an internal state variable. This approach retains the state-space formulation for explicit identification and validation from flight data. Greenwell [13] provides a review of unsteady aerodynamic modeling whereas Refs [14 and15] present the application of the same to flight data.

Aerodynamics pertaining to static attached flow conditions can be adequately modeled using time-invariant aerodynamic parameters and linear models. Output error method and its variants are routinely used to extract aerodynamic model pertaining to stationary attached flow conditions. But in case of detached flow conditions at high angles of attack near stall, the aerodynamic forces and moments become highly nonlinear and are associated with noticeable unsteady effects. The application of output error method and its variants [16-18] for parameter estimation using flight data of air vehicle require postulation of correct flight dynamic formulations having accurate description of aerodynamic model. Since aerodynamic model at high angles of attack near stall may not be exact, the solution of equations of motion using in-exact aerodynamic model may lead to inaccurate computation of response of motion variables (modeling error). This modeling error, if limited, can be treated as process noise. Most of the estimation methods (output error method and its variants) face difficulties in estimating aerodynamic parameters from flight data having process noise.

More recently, investigations have been carried out to explore the potential of Artificial Neural Networks [19-25] for aircraft aerodynamic modeling and parameter estimation. Feed Forward Neural Network (FFNN) is found to be the most promising for its application to aircraft modeling. The main advantage and strength of FFNN [19-25] modeling is in its ability to capture highly nonlinear complex phenomena for which the model postulation with physical understanding is difficult. It has been shown that FFNN can work as general function approximators and thereby are capable of approximating any continuous function to any desired accuracy provided the appropriate number of hidden layers and the neurons per layer exist and that the activation function is continuous. It has been shown [10] during the modeling of lift, drag and pitching moment coefficients of the research aircraft HFB-320 that the predictive capability of the trained FFNN for flight data with atmospheric turbulence is found to be good. The capability of FFNN to model highly nonlinear complex phenomena and handle the process noise in a better way has been utilized to estimate the aerodynamic parameters from flight data at high angles of attack in the presented work.

In the present work, Neural Gauss-Newton method (NGN), proposed by Peyada [24-25] has been used for aerodynamic parameter estimation from real flight data of Hansa-3 aircraft at high angles of attack near stall. The NGN method uses input and output variables directly from the measured real flight data for the task of parameter estimation. Therefore, the method bypasses the solving of equations of motion and hence, the involvement of any inaccuracies due to unsteady effects, aerodynamic model (not so exact) in computing estimated response.

The use of Kirchhoff's quasi-steady stall model [10] was made to include unsteady effects in the aerodynamic model, thereby making the estimation model nonlinear. The nonlinear longitudinal aerodynamic model used for parameter estimation consisted of lift, drag and pitching moment coefficients which included unsteady effects in terms of flow separation point and hysteresis derivatives. The flow separation point is a function of static stall characteristics, break point and time constant.

The NGN method, first validated on flight data at moderate angles of attack, was implemented on flight data at high angles of attack. Encouraging results were obtained in the form of longitudinal aerodynamic and stall characteristic parameters. These estimates when compared with Maximum Likelihood (ML) estimates proved the supremacy of the NGN method.

In the presented work, in Section - Real Flight Data Generation and Data Compatibility Check, explains the procedure for generation and processing of real flight data and highlights the conduct of flight tests using Hansa-3 aircraft. Data compatibility check has also been carried out in the same section. Description regarding quasi-steady stall modeling has been presented in Section - Quasi-steady Stall Modeling. Linear and nonlinear aerodynamic models used for parameter estimation are given in Section - Aerodynamic Models used for parameter Estimation. The procedure for application of NGN method has been presented in Section - Neural-Gauss-Newton Method. Results have been presented and discussed in Section - Results and Discussion. Concluding remarks along with scope for future work have been highlighted in the conclusion section.

Real Flight Data Generation and Data Compatibility Check

A flight test program using Hansa-3 (Fig.1), an in-house fully instrumented research aircraft, was conducted at Flight Laboratory of Indian Institute of Technology, Kanpur to gather the real flight data with the help of data acquisition system. The data was gathered corresponding to 3-2-1-1, doublet and quasi-steady stall maneuver (QSSM). The elevator from trim condition was deflected by the pilot to execute 3-2-1-1, doublet and well designed QSSM. However, the execution of 3-2-1-1 and doublet maneuvers was not difficult as the control deflections were limited to generate the response of motion variables at moderate angles of attack. But, the execution of QSSM was not an easy task as the control deflection involved high angles of attack near stall. In spite of a lot of efforts, only one set of flight data corresponding to QSSM, that reasonably represented the nonlinear characteristics, could be generated.

An onboard measurement system installed on the test aircraft provided the measurements of large number of signals such as aircraft motion variables, atmospheric conditions, control surface position etc. using dedicated sensors. The measurements made in flight were recorded on board at a sampling rate of 50 Hz using suitable interface with standard Laptop. The flight data consisted of raw data for measured V, α, β, p, q, r, a_x, a_y, a_z, φ, θ, ψ, h, δ_a, δ_e and δ_r and the location of measuring sensors. The measurements of V, α and β were obtained with flight log mounted on a boom fixed to the tip of the wing.

The accelerations (a_x , a_y , a_z) along the three body axes were measured using an accelerometer located near the centre of gravity of the aircraft. The angular rates (p, q and r) were obtained from the measurements available from the inertial platform. The angular accelerations ($\dot{p}$, $\dot{q}$ and $\dot{r}$) were obtained by numerical differentiation of the corresponding angular rates (p, q and r). The control surface deflections (δ_a , δ_e and δ_r) were measured using potentiometer. The temperature T was recorded using the standard cockpit outside air temperature (OAT) gauze.

After establishing a typical cruise at desired altitude, elevator was deflected to excite longitudinal dynamics of Hansa-3 using 3-2-1-1, doublet and QSSM. Three real flight data sets consisting of time histories of various measured states and motion variables were generated. Figs.(2-4) present the flight data in terms of angle of attack (α), pitch angle (θ), pitch rate (q), velocity (V) and acceleration along x- and z-axis (a_x and a_z). The variables α, β, ϕ, θ, ψ and δ_e used in plots are in degrees whereas the variables a_x, and a_z are in m/s^2. The variables V, h and q are in m/s, m and deg/s, respectively.

Figures 2 and 3 show that a negative elevator deflection (Trailing edge deflected upwards) from trim condition leads to increase in α, θ, q, a_x (a measure of drag) and a_z (a measure of lift coefficient) whereas the trend of variation gets reversed when the deflection is in the opposite direction. It can also be observed that there is a continuous increase and decrease in V even at trim condition for 3-2-1-1 and doublet input respectively. This increase or decrease may be due to not so-exact trim achieved during the flight test. However, the velocity reduces as the elevator is deflected in negative direction (3-2-1-1 input) and increases as the elevator is deflected in positive direction (doublet input) from trim condition. Since the maneuver was so quick, the trend of variation for the following deflections was difficult to ascertain.

Data set corresponding to 3-2-1-1 control input (Fig.2) was used to estimate aerodynamic parameters with a purpose to validate NGN method at moderate angles of attack. Doublet control input (Fig.3) was used to validate NGN estimates obtained from data set corresponding to 3-2-1-1 input.

Figure 4 presents the state and motion variables corresponding to quasi-steady stall maneuver. This data set was used to model the nonlinear aerodynamics and estimate parameters using NGN method and Kirchhoff's quasi-steady stall model.

Figure 4 shows that the maximum angle of attack (α_{max}) of 18 degrees was achieved during the execution of QSSM. A sudden change in the value of a_z, a measure of lift (C_L), confirms a drop in lift coefficient beyond α_{max}. A sudden drop in C_L beyond 18 degrees establishes the occurrence of stall phenomena. The horizontal acceleration (a_x), representing the drag characteristics, shows that the drag increases drastically during the stall. All other variables also vary in a manner in which they should vary during the execution of such maneuver. The pitch angle (θ) dips drastically and even touches -18 degrees during the maneuver. Similarly sudden change in pitch rate (q) is observed near the stall region. The speed (V) of aircraft keeps on increasing as long as the pitch angle keeps on decreasing. The flight data confirms to the expectation of the behavior of almost near stall. These data were used to capture nonlinear aerodynamics near stall using NGN method and Kirchhoff's quasi-steady stall model. Table-1 presents the geometrical characteristics of Hansa-3 aircraft used to carry out the study.

Table-1 : Geometrical Characteristics of Hansa-3 Aircraft

Component (Symbol)	Value (Units)
Aircraft Mass (m)	750 (Kg)
Wing Planform Area (S)	12.47 (m^2)
Aspect Ratio (A)	8.8
MAC ($\bar{c}$)	1.21 (m)
Span (b)	10.47 (m)

Data compatibility check [10] also referred as Flight path reconstruction (FPR) was carried out to ensure that the measurements used for subsequent aerodynamic model identification were consistent and error free. The scale factors, zero shifts and time delays present in the measured flight variables are estimated using observation equations and Maximum Likelihood (ML) algorithm. The following set of unknown parameters was considered adequate for reconstructing the longitudinal dynamics of Hansa-3 aircraft for data compatibility check.

$$\Theta = \left[\Delta a_x \;\; \Delta a_y \;\; \Delta a_z \;\; \Delta p \;\; \Delta q \;\; \Delta r \;\; K_\alpha \;\; \Delta \alpha \right]^T \qquad (1)$$

Figure 5 presents the measured and computed response of motion variables during compatibility check using flight data pertaining to QSSM. Data compatibility check was carried out on all three data sets (Table-2), but the graphical result has been presented only for QSSM.

It was observed that the matching of measured and estimated response was slightly better for the real flight data corresponding to 3-2-1-1 and doublet input (not shown) than in case of quasi-steady stall maneuver (Fig.5).

Ideally, the scale factors close to unity and negligible biases suggest the high accuracy of the gathered flight data. Table-2 presents the estimated scale factor and biases for all the three sets of real flight data along with the values of Cramer-Rao bounds. It can be observed from the estimated values that the biases are negligible and scale factor is close to unity for 3-2-1-1 and doublet input establishing the high accuracy of estimation. In case of quasi-steady stall maneuver, the biases are negligible but the scale factor departs slightly from unity. This may be due to distorted position of sensors during the execution of maneuver leading to slightly inaccurate capturing of the real flight data.

Table-2 : Data Compatibility Check for Longitudinal Real Flight Data of Hansa-3 Aircraft

Factors → Input ↓	Δa_x (m/s^2)	Δa_y (m/s^2)	Δa_z (m/s^2)	Δp (rad/s)	Δq (rad/s)	Δr (rad/s)	$K\alpha$	$\Delta\alpha$ (rad)
3-2-1	0.080 (0.080)	-0.026 (0.001)	0.001 (0.001)	-0.0007 (0.0)	-0.0009 (0.0)	0.003 (0.0)	1.02 (0.008)	-0.004 (0.0)
Doublet	-0.181 (0.001)	0.172 (0.001)	0.014 (0.001)	0.001 (0.0)	-0.0009 (0.0)	-0.002 (0.0)	0.0983 (0.011)	0.001 (0.002)
QSSM	-0.839 (0.002)	-0.045 (0.002)	-0.025 (0.0)	-0.0007 (0.0)	-0.0004 (0.0)	0.0048 (0.0)	0.627 (0.003)	0.119 (0.0)

( ) Cramer-Rao Bounds

Quasi-steady Stall Modeling

Aerodynamic models become highly nonlinear due to dominant unsteady effects and flow separation at higher angles of attack and aircrafts undergoing stall. For such a case, a non-dimensional state X describes the instantaneous location of an idealized flow separation point along the chord on the upper surface of the wing ($0 \le X \le 1$), where X=1 and X=0 correspond to attached and fully separated flow respectively. Kirchhoff's flow separation theory, for a symmetrical profile, can be used to model the wing lift [10] as a function of angle of attack (α) and flow separation point (X) with the help of Eq.2.

$$C_L(\alpha, X) = C_{L_\alpha}\left\{\frac{1+\sqrt{X}}{2}\right\}^2 \alpha$$

where

$$C_{L_\alpha} = \frac{(2\pi A)}{\left(2+\sqrt{4+\frac{A^2\beta^2}{\eta^2}(1+\frac{\tan^2\Lambda}{\beta^2})}\right)} * \frac{S_{exposed}}{S_{ref}} \quad (2)$$

Reformulation of the Kirchhoff's expression (Eq.2) for non-symmetrical profile gives [10]:

$$X_o = \left\{2\sqrt{[(C_L - C_{L_o})/(C_{L_\alpha}\alpha)]} - 1\right\}^2 \quad (3)$$

The steady flow separation point (X_o) depends upon the airfoil and wing configuration. Using Eq.(2) with X=Xo, the function can be determined statically in wind tunnel. Using the following approximation based on hyperbolic tangent [10]:

$$X_o = \frac{1}{2}\left\{1 - \tan h\ [a_1(\alpha - \alpha^*)]\right\} \quad (4)$$

Where a_1 defines the static stall characteristics of the airfoil and α^* the breakpoint corresponding to $X_o = 0.5$. This approximation is better suited to parameter estimation because it is a continuous function in its entire range and has just two unknown parameters, namely a_1 and α^*.

The general representation [10] for unsteady flow characterizing the transient and quasi-steady effects is given by Eq.5.

$$\tau_1 \frac{dX}{dt} + X = \frac{1}{2}\left\{1 - \tan h\ [a_1(\alpha - \tau_2\dot{\alpha} - \alpha^*)]\right\} \quad (5)$$

Although Eq.(5) provides a model characterizing both the transient and quasi-steady stall characteristics in terms of four parameters, namely a_1, α^*, τ_1 and τ_2, estimation of these parameters requires appropriate flight maneuvers containing adequate information necessary to estimate each parameter separately. Determination of both the time constants (τ_1 and τ_2) requires highly dynamic stall maneuvers. Flight data with dynamic stall is more difficult and risky to gather, whereas it is relatively easier to perform quasi-steady stall maneuver. This simplified approach accounting for quasi-steady stall characteristics is considered adequate. Flight data with quasi-steady stall would enable estimation of the hysteresis time constant τ_2 only. Accordingly, the transient effects can be neglected by setting τ_1 equal to zero. This eliminates the need of differential equation and Eq.(5) simplifies to [10]:

$$X = \frac{1}{2}\left\{1 - \tan h\ [a_1(\alpha - \tau_2\dot{\alpha} - \alpha^*)]\right\} \quad (6)$$

Aerodynamic Models used for Parameter Estimation

The following aerodynamic model was used for longitudinal parameter estimation from flight data of Hansa-3 aircraft pertaining to 3-2-1-1 input using NGN and ML methods.

$$C_D = C_{D_o} + C_{D_\alpha}\alpha + C_{D_{\delta e}}\delta_e \tag{7.1}$$

$$C_L = C_{L_o} + C_{L_\alpha}\alpha + C_{L_q}(q\bar{c}/2V) + C_{L_{\delta e}}\delta_e \tag{7.2}$$

$$C_m = C_{m_o} + C_{m_\alpha}\alpha + C_{m_q}(q\bar{c}/2V) + C_{m_{\delta e}}\delta_e \tag{7.3}$$

The aerodynamic model used for parameter estimation from real flight data pertaining to quasi-steady stall maneuver is given by Eqs.(8.1-8.3).

$$C_L = C_{L_o} + C_{L_\alpha}\left\{\frac{1+\sqrt{X}}{2}\right\}^2\alpha \tag{8.1}$$

$$C_D = C_{D_o} + \frac{1}{e\pi A}C_L^2 + \frac{\partial C_D}{\partial X}(1-X) \tag{8.2}$$

$$C_m = C_{m_o} + C_{m_\alpha}\alpha + C_{m_q}\frac{q\bar{c}}{2V} + C_{m_{\delta e}}\delta e + \frac{\partial C_m}{\partial X}(1-X) \tag{8.3}$$

where A, e, δ_e and q are the wing aspect ratio, Oswald factor, elevator deflection and pitch rate respectively. Any additional effects are accounted for through an empirical correction term $\frac{\partial C_D}{\partial X}$. The parameter $\frac{\partial C_m}{\partial X}$ models any hysteresis effect in the pitching moment.

The aim was to estimate unknown parameter vectors [ζ (Eq.9) and ξ (Eq.10)] from real flight data pertaining to 3-2-1-1 and QSSM, respectively.

$$\zeta = \left[C_{D_o}\ C_{D_\alpha}\ C_{D_{\delta e}}\ C_{L_o}\ C_{L_\alpha}\ C_{L_q}\ C_{L_{\delta e}}\ C_{m_o}\ C_{m_\alpha}\ C_{m_q}\ C_{m_{\delta e}}\right]^T \tag{9}$$

$$\xi = \left[a_1\ \tau_2\ \alpha^*\ C_{D_o}\ C_{D_X}\ C_{L_o}\ C_{L_\alpha}\ C_{m_o}\ C_{m_\alpha}\ C_{m_q}\ C_{m_{\delta e}}\ C_{m_X}\right]^T \tag{10}$$

Table-3 presents the wind tunnel values of parameters for Hansa-3 aircraft which were used as a reference to compare the estimated results.

Table-3 : Wind Tunnel Values of Aerodynamic Parameters

Parameters	Wind Tunnel Value
C_{D_o}	0.035
C_{D_α}	0.086
$C_{D_{\delta e}}$	0.026
C_{L_o}	0.354
C_{L_α}	4.978
$C_{L_{\delta e}}$	0.265
C_{m_o}	0.052
C_{m_α}	-0.496
$C_{m_{\delta e}}$	-1.008

Neural-Gauss-Newton Method

The NGN method is an algorithm that utilizes the FFNN and Gauss-Newton optimization to estimate the aerodynamic parameters. The neural model has been used to predict time histories of motion variables at $(k+1)^{th}$ instant given the measured initial conditions corresponding to k^{th} instant (where k = 1 to n: n is the total number of discrete data points). It has been observed that for all practical purposes of parameter estimation, this approach helps in building flight dynamic model (in restricted sense) using measured input-output data and does not require any priori postulation of mathematical model or solving of equations of motion. Fig.6 presents the neural-architecture for longitudinal flight dynamic model.

Let the measured flight data contains the time histories of $\alpha(k)$, $\theta(k)$, $q(k)$, $V(k)$, $a_x(k)$, $a_z(k)$ at k^{th} instant. Next step is to form the input $U(k)$ and the output $Z(k+1)$ vectors for building the aircraft dynamic model using neural network architecture as given in Fig.6.

The input vector, $U(k)$ required to build flight dynamic model can be defined as:

$$U(k) = \left[\alpha(k)\ \theta(k)\ q(k)\ V(k)\ C_D(k)\ C_L(k)\ C_m(k)\right]^T \tag{11}$$

The values of $C_D(k)$, $C_L(k)$ and $C_m(k)$ at the k^{th} instant can be obtained by plugging measurement variables $\alpha(k)$, $a_x(k)$, $a_z(k)$ and dynamic pressure $\bar{q}(k)$ along with mass and inertia characteristics in Eqs.(12.1-12.3).

$$C_D(k) = -C_X(k)\cos\alpha(k) - C_Z(k)\sin\alpha(k) \quad (12.1)$$

$$C_L(k) = -C_X(k)\sin\alpha(k) - C_Z(k)\cos\alpha(k) \quad (12.2)$$

$$C_m(k) = \begin{bmatrix} I_y \dot{q}(k) - I_{xz}(p^2(k) - r^2(k)) - (I_z - I_x)(p(k)\, r(k)) \\ -F_{eng}\cos\sigma_{eng} Z_{ENCG} - F_{eng}\sin\sigma_{eng} Y_{ENCG} \end{bmatrix} \Big/ (\bar{q}(k)\, S\, \bar{c}) \quad (12.3)$$

where $C_X(k)$ and $C_Z(k)$ can be computed using Eqs.(13.1-13.2).

$$C_X(k) = ma_x^{CG}(k)/(\bar{q}(k)\, S) \quad (13.1)$$

$$C_Z(k) = ma_Z^{CG}(k)/(\bar{q}(k)\, S) \quad (13.2)$$

The output vector $Z(k+1)$ at $(k+1)^{th}$ instant required for building flight dynamic model be constructed as per Eq.(14).

$$Z(k+1) = \left[\alpha(k+1)\ \theta(k+1)\ q(k+1)\ V(k+1)\ a_x(k+1)\ a_z(k+1)\right]^T \quad (14)$$

Since the neural mapping uses measured motion variables, the performance and applicability of the method can also be influenced by data quality. The selection of number of iteration and number of neuron in hidden layer plays an important role during neural modeling while handling flight data with noise.

The algorithm of NGN method can be summarized with the help of Fig.7 as follows:

a) As a first step, the measured flight data undergoes data compatibly check. The measured motion variables are then transferred to center of gravity for further use during estimation process (Block: 1-3 of Fig.7).

b) The procedure followed for neural training using FFNNs is explained in blocks 3-8.

c) Block 9 checks the convergence criteria for FFNNs training. Once training is accomplished the trained neural model is used for parameter estimation.

d) Once aerodynamic model is chosen, the already trained neural model is used to calculate system output $Y(k)$. Input $U(k)$ is constructed in block 10 using aerodynamic model fed through block 15. The input $U(k)$ is fed to block 5 to estimate system output $Y(k)$.

e) The computed response Y(k) and $\partial Y(k)/\partial\Theta$ (from block 11) (where $\Theta = \zeta, \xi$) are fed to block 12 and 13 to update aerodynamic parameter. The aerodynamic model is updated using this new set of aerodynamic parameters in block 15. The computation through steps (d) to (e) is continued till the convergence criterion (block 14) is achieved. Once convergence is achieved, parameters are estimated along with associated standard deviation.

Results and Discussion

First, the suitability of NGN method for parameter estimation was ascertained through the application of the method on the data pertaining to 3-2-1-1 control input. The estimates obtained using NGN were compared with ML estimates to establish the method. The estimates were also validated using doublet control input. The established NGN algorithm was, then, applied to the real flight data gathered using QSSM for nonlinear aerodynamic modeling and parameter estimation.

Parameter Estimation from Real Flight Data: 3-2-1-1 Input

The NGN algorithm was applied to real flight data pertaining to 3-2-1-1 elevator control input with a motive to establish NGN method for parameter estimation. The aim was to estimate unknown parameter vector (ζ) consisting of aerodynamic parameters namely, $C_{D_o}\ C_{D_\alpha}\ C_{D_{\delta e}}\ C_{L_o}\ C_{L_\alpha} \ldots \ldots\ C_{m_{\delta e}}$ as given in Eq.(9). The neural model was developed using input vector $U(k)$ and output vector $Z(k+1)$ for longitudinal parameter estimation. The input vector $U(k)$ was reconstructed by keeping the same initial conditions $\alpha(k)$, $\theta(k)$, $q(k)$, $V(k)$ used for training, however, $C_D(k)$, $C_L(k)$ and $C_m(k)$ corresponding to identical control input, used for generating flight data, were modified as per the aerodynamic model in the estimating algorithm.

To start the estimation algorithm, it was necessary to specify some suitable initial guess values of the unknown parameters vector (ζ), consisting of non-dimensional parameters used for the description of aerodynamic model of $C_D(k)$, $C_L(k)$ and $C_m(k)$. Using the initial guess values of the aerodynamic parameters, the coefficients

C_{D_e}, C_{L_e} and C_{m_e} were computed. Next, the estimated response of the aircraft $Y(k+1)$ at $(k+1)^{th}$ instant was computed using input vector $U(k)$ having same measured flight data with $C_D(k)$, $C_L(k)$ and $C_m(k)$ replaced by C_{D_e}, C_{L_e} and C_{m_e}. Let this estimated response be represented by output vector as given below.

$$Y(k+1) = \left[\alpha(k+1)\ \ \theta(k+1)\ \ q(k+1)\ \ V(k+1)\ \ a_x(k+1)\ \ a_z(k+1)\right]^T$$

Next, the residual error $E(k)$ between measured flight data $Z(k+1)$ and neural output $Y(k+1)$ was minimized to estimate the unknown parameter vector (ζ). the residual error $E(k)$ and covariance matrix of the residual (R) were computed using Eqs.(15-16).

$$E(k) = [Z(k) - Y(k)] \tag{15}$$

$$R = \frac{1}{N}\sum_{k=1}^{N}[Z(k) - Y(k)]\ [Z(k) - Y(k)]^T \tag{16}$$

The cost function to be minimized using maximum likelihood method to estimate ζ is given by Eq.(17).

$$J(\zeta, R) = \frac{1}{2}\sum_{k=1}^{N}[Z(k) - Y(k)]^T R^{-1}\ [Z(k) - Y(k)] \tag{17}$$

The terms R, $Z(k)$ and $Y(k)$ are defined as measurement covariance matrix, measured and estimated output at k^{th} instant respectively.

Input vector $U(k)$ consisted of time histories at k^{th} instant of variables $\alpha(k)$, $\theta(k)$, $q(k)$, $V(k)$, $C_D(k)$, $C_L(k)$ and $C_m(k)$ whereas the output vector, Z(k+1) had $\alpha(k+1)$, $\theta(k+1)$, $q(k+1)$, $V(k+1)$, $a_x(k+1)$, $a_z(k+1)$ as its elements. These two input-output vectors were used to train the neural model shown in Fig.7.

The FFNN used a log-sigmoid and linear transfer function as the activation function and Levenberg-Marquardt algorithm was used for updating the neural network weights. The mean square error criterion or the number of iterations decided the termination of the iterative process. A range of values of the network parameters was tried to arrive at the final architecture of FFNN used for neural modeling. The final FFNN structure consisted of one hidden layer having five neurons with learning rate of 0.3 and the number of iterations equal to 4000. The network parameters finally chosen gave a good match between the true and the predicted values of the time histories of the variables.

Figure 8 shows a well matched comparison of measured and trained response of various state and motion variables obtained during the training process for flight data of Hansa-3 aircraft pertaining to 3-2-1-1 control input. After successful training of the neural model, the parameters (Eq. 9) were estimated by minimizing the error cost function $J(\zeta, R)$ using ML method following the procedure explained in the previous section. Fig.9 presents a well matched comparison of measured and estimated response of various state and motion variables obtained during the estimation process for flight data pertaining to 3-2-1-1 control input.

Table-4 presents the estimated aerodynamic parameters from real flight data pertaining to 3-2-1-1 input using NGN and maximum likelihood (ML) methods. It can be observed that the estimated values of aerodynamic pa-

Table-4 : Parameter Estimates Using 3-2-1-1 Input

Derivatives	ML	NGN
C_{D_o}	0.076 (1.1e-4)	0.07 (2.9e-3)
C_{D_α}	0.083 (1.1e-2)	0.087 (2.1e-2)
$C_{D_{\delta e}}$	0.010 (1.0e-2)	0.062 (2.1e-2)
C_{L_o}	0.068 (4.7e-3)	0.28 (5.6e-3)
C_{L_α}	5.813 (3.0e-2	5.528 (3.8e-2)
C_{L_q}	2.679 (1.5e+0)	23.84 (1.7e+0)
$C_{L_{\delta e}}$	0.450 (5.6e-2)	1.233 (6.4e-2)
C_{m_o}	0.094 (4.1e-4)	0.128 (8.1e-3)
C_{m_α}	-0.458 (1.9e-3)	-0.564 (5.5e-2)
C_{m_q}	-8.205 (1.3e-1)	-6.983 (2.5e+0)
$C_{m_{\delta e}}$	-0.772 (5.2e-3)	-0.961 (9.4e-2)

( ) Cramer-Rao Bounds

rameters using NGN method compares well with the values estimated using ML (Table-4) as well as with the wind tunnel values (Table-3) except for the parameters C_{D_o}, $C_{L_{\delta e}}$ and C_{m_o} which are slightly of higher magnitude. It has been observed that the parameters C_{L_q} and $C_{L_{\delta e}}$ are weak derivatives and have negligible effect on aircraft motion.

To gain more confidence on the method, the estimates from NGN were used to carry out the validation process using doublet input. The estimates obtained from real flight data pertaining to 3-2-1-1 input were used to generate the response of various state and motion variables using six degrees of freedom (DOF) model and doublet elevator control input with initial conditions of the measured data. This generated response was compared with the measured response of state and motion variables pertaining to doublet elevator input.

Figure 10 presents a comparison between the measured response and the response for doublet control input generated by using estimates obtained from 3-2-1-1 control input using ML and NGN methods. A reasonably good match between the two responses validates NGN method for the parameter estimation at low/moderate angles of attack.

Nonlinear Aerodynamic Modeling Using Real Flight Data: QSSM

Next, the real flight data at high angles of attack near stall pertaining to a well designed quasi-steady stall maneuver was used to model nonlinear aerodynamics. Aerodynamic model incorporated with unsteady effects at high angles of attack using Kirchhoff's quasi-steady stall model was utilized to estimate the stall characteristics and aerodynamic parameters. Now, the aim was to estimate unknown parameter vector ξ consisting of aerodynamic parameters namely, a_1 τ_2 α^* C_{D_o} C_{D_X} C_{L_o} ... ... C_{m_X} as given in Eq.(10). Both, ML and NGN methods were applied to compatible flight data pertaining to QSSM for the estimation of aerodynamic and stall characteristic parameters.

In a similar fashion as in the case of 3-2-1-1 control input, the neural model was trained for the data pertaining to QSSM by varying the network parameters one by one. The final FFNN structure consisted of one hidden layer with five neurons with learning rate of 0.35 and the number of iterations equal to 4000. Fig.11 shows a well matched comparison of measured and trained response of motion variables obtained during the training process using flight data pertaining to QSSM.

After successful training of the neural model, the parameter vector, ξ (Eq.10) was estimated by minimizing the error cost function $J(\xi, R)$ using ML method following the procedure explained in the previous section.

Figure 12 presents a comparison of measured and estimated response of various state and motion variables obtained during the estimation process for flight data pertaining to quasi-steady stall maneuver. It can be observed that the matching for angle of attack (α), pitch rate (q) and velocity (V) is quite good but the matching for other variables (θ, a_x and a_z) is slightly poor.

Table-5 presents the estimated aerodynamic parameters and the parameters characterizing stall characteristics from real flight data pertaining to quasi-steady stall maneuver using NGN method. Table-5 also presents the parameters for ATTAS and Hansa-3 aircraft using ML method. It can be observed that the estimated values (Table-5) of most of the aerodynamic parameters using NGN method are in close agreement with the wind tunnel values (Table-3) except for the parameters C_{m_o} and C_{m_q}. The value of the parameter C_{m_q} could not be estimated correctly while the value of C_{m_o} was slightly of lower magnitude. It can also be observed that most of the parameters characterizing stall characteristics (a_1, τ_2, and C_{D_X}) were having reasonable values as compared to ATTAS(10) aircraft results. However, the value of parameter C_{m_X} could not be estimated correctly as it gave positive value. Most of the parameters followed the trend in terms of sign and value. The lacking in the accurate estimation may be attributed to the not so good quality of data gathered (due to distorted orientation of probes) during flight testing.

Conclusion

The work presented the modeling of nonlinear aerodynamic for Hansa-3 aircraft using NGN method. The use of Kirchhoff's quasi-steady stall model made to include the unsteady effects in the aerodynamic model. First, NGN method was applied to real flight data gathered at moderate angles of attack using 3-2-1-1 elevator control input. Reasonably good estimates established the NGN method for

Table-5 : Parameter Estimation Using Quasi-Steady Stall Maneuver

Derivatives	ML (ATTAS)	ML (Hansa-3)	NGN (Hansa-3)
a_1	23.71 (8.1e-1)	55.45 (3.6e+0)	13.51 (2.8e-1)
τ_2	24.02 (3.5e-1)	65.15 (4.7e+0)	16.20 (1.0e-0)
α^* (deg)	17.64 (1.1e-3)	15.01 (1.1e-3)	10.31 (2.3e-3)
C_{D_o}	0.043 (4.3e-4)	0.113 (3.1e-3)	0.044 (1.7e-3)
C_{L_o}	0.157 (3.2e-3)	0.585 (8.9e-3)	0.474 (2.7e-3)
C_{L_α}	3.3. (3.7e-2)	4.7 (7.8e-2)	5.5 (7.0e-2)
C_{m_o}	0.050 (1.7e-3)	0.019 (6.6e-4)	0.028 (2.7e-3)
C_{m_α}	-0.176 (1.1e-2)	0.063 (5.7e-3)	-0.602 (7.0e-2)
C_{m_q}	-6.371 (2.7e-1)	0.371 (4.3e-1)	48.64 (2.4e+0)
$C_{m_{\delta e}}$	0.39 (1.6e-1)	0.009 (6.1e-3)	-0.158 (3.0e-2)
C_{D_X}	0.079 (3.0e-3)	-0.071 (5.5e-3)	0.005 (4.2e-3)
C_{m_X}	-0.12 (5.0e-3)	-0.018 (1.4e-3)	0.123 (1.7e-2)

( ) Cramer-Rao Bounds

parameter estimation at moderate angles of attack (linear models). Next, the method was successfully implemented on the nonlinear data to model the nonlinear aerodynamics of Hansa-3 aircraft using Kirchhoff's quasi-steady stall model. It was observed that most of the estimated parameters followed the desired trend in terms of sign and magnitude of estimated values. The departure between the measured and estimated results in case of few parameters may be attributed to the inappropriate attitude of the of angle of attack and sideslip vanes during the dynamic maneuver executed during the conduct of flight test. For future scope of work, it is suggested that NGN method for modeling nonlinear aerodynamics using Kirchhoff's quasi-steady stall model can be established in a more authentic manner if sufficient real flight data of high accuracy at high angles of attack near stall could be generated.

References

1. Hamel, P. G. and Jategaonkar, R. V., "The Evolution of Flight Vehicle System Identification", AGARD, DLR Germany, 8-10, May, 1995.

2. Iliff, K. W., "Parameter Estimation for Flight Vehicle", Journal of Guidance, Control and Dynamics, Vol.12, No.5, 1989, pp.609-622.

3. Hamel, P. G., "Aircraft Parameter Identification Methods and their Applications Survey and Future Aspects", AGARD, 15-104, Nov,1979, Paper 1.

4. Klein, V., "Estimation of Aircraft Aerodynamic Parameter from Flight Data", Progress in Aerospace Sciences, Vol. 26, No. 1, 1989, pp. 1-77.

5. Maine, K. E. and Iliff, K. W., "Application of Parameter Estimation to Aircraft Stability and Control: The Output Error Approach", NASA RP 1168, Jan, 1986.

6. Maine, R. E. and Iliff, K. W., "Identification of Dynamic Systems - Application to Aircraft - Part 1: Output Error Approach", AGARD-AG-300, Vol. 3, Part 1, Dec, 1986.

7. Greenberg, H., "A Survey of Methods for Determining Stability Parameters of an Airplane from Dynamic Flight Measurements", NACA TN-2340, April 1951.

8. Roskam, J., "Methods for Estimating Stability and Control Derivatives for Conventional Subsonic Airplanes", Roskam Aviation and Engineering Corporation, 1973.

9. Klein, V. and Morelli, E. A., "Aircraft System Identification - Theory and Practice", AIAA Education Series, Inc., Reston, Virginia, 2006.

10. Jategaonkar, R. V., "Flight Vehicle System Identification - A Time Domain Methodology", AIAA Progress in Aeronautics and Astronautics, Vol. 216, AIAA, Reston, VA, Aug, 2006.

11. Goman, M. and Khrabrov, A., "State-space Representation of Aerodynamic Characteristics of an Aircraft at High Angles of Attack", J. of Aircraft, Vol.31, No. 51, pp.990.

12. Leishman, J.G. and Naguyen, K.Q., "State-space Representation of Unsteady Airfoil Behavior", AIAA Journal, Vol. 28, No. 5, 1990, pp. 836-844.

13. Aerodynamic Greenwell, D. I., "A Review of Unsteady Aerodynamic Modeling for Flight Dynamics of Manoeuvrable Aircraft", AIAA Paper, 2004-5276, 2004.

14. Fischenberg, D., "Identification of an Unsteady Aerodynamic Stall Model from Flight Test Data", AIAA Paper, 95-3438, 1995.

15. Fischenberg, D. and Jategaonkar, R. V., "Identification of Aircraft Stall Behavior from Flight Test Data", RTO-MP-11, Paper No. 17, 1999.

16. Shinbrot, M., "A Least square Curve Fitting Method with Applications to the Calculation of Stability Coefficients from Transient Response Data", NACA TN 2341, April, 1951.

17. Mehra, R. K., "Maximum Likelihood Identification of Aircraft Parameters", Proceedings of the 11th Joint Automatic Control Conference, Atlanta, GA, 1970.

18. Jategaonkar, R. V. and Plaetschke, E., "Estimation of Aircraft Parameters Using Filter Error Methods and Extended Kalman Filter", DFVLR-FB 88-15, March, 1988.

19. Zurada, J. M., "Introduction to Artificial Neural Systems", West, New York, 1992.

20. Haykins, S., "Neural Networks - A Comprehensive Foundation", McMaster University, Macmillan College Publishing Company, New York, 1994.

21. Hassoun, M. H., "Fundamental of Artificial Neural Networks", The MIT Press, Cambridge, MA, 1995.

22. Basappa, K. and Jategaonkar, R. V., "Aspects of Feed Forward Neural Network Modeling and its Application to Lateral-Directional Flight-Data", DLR IB 111-95/30, Sept, 1995.

23. Ghosh, A. K., "Aircraft Parameter Estimation from Flight Data using Feed Forward Neural Networks", PhD Thesis, Department of Aerospace Engineering, Indian Institute of Technology, Kanpur, April, 1998.

24. Peyada, N. K. and Ghosh, A. K., "Parameter Estimation from Real Flight Data using Neural Network based Method", INCPAA-2008, Mathematical Problems in Engineering, Aerospace and Sciences, University of Genoa, Italy, June, 25-27, 2008.

25. Peyada, N. K. and Ghosh, A. K., "Aircraft Parameter Estimation using New Filtering Technique Based on Neural Network and Gauss-Newton Method", Aeronautical Journal, UK, Vol.113, No. 1142, April, 2009.

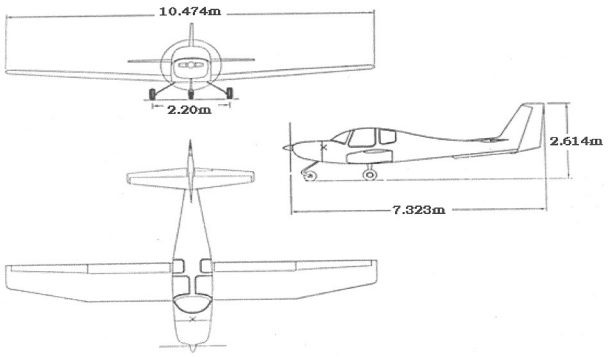

Fig.1 Plan Form of Hansa-3 Aircraft

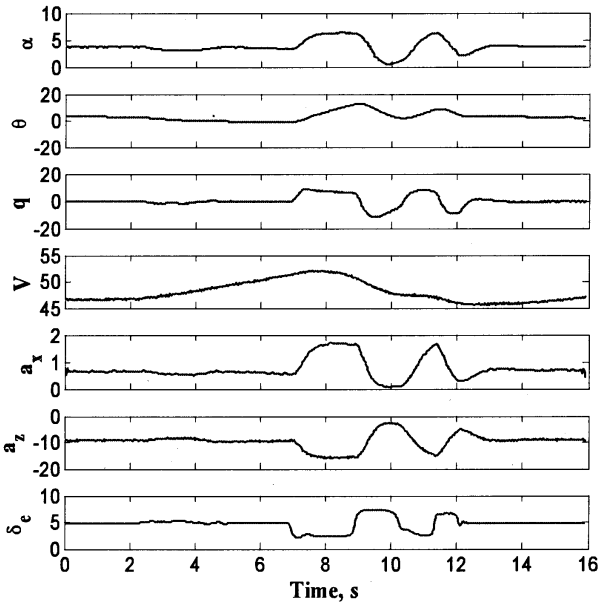

Fig.2 Real Flight Data : 3-2-1-1 Elevator Control Input

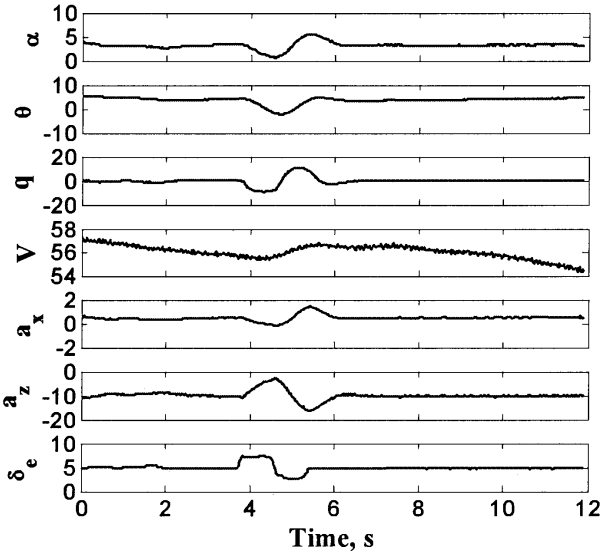

Fig.3 Real Flight Data : Doublet Elevator Control Input

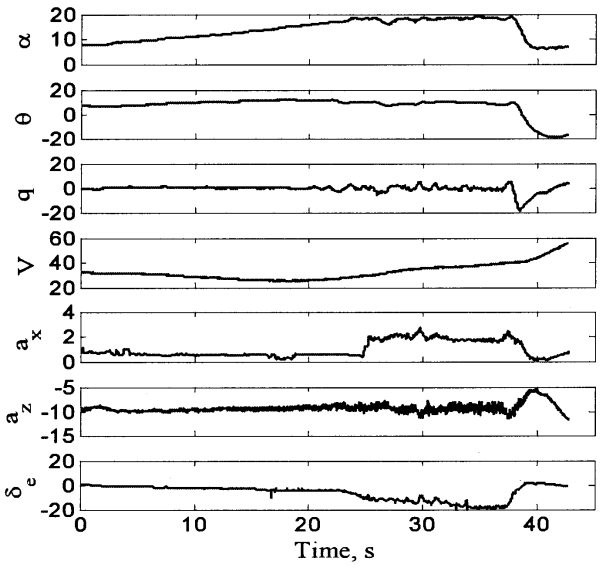

Fig.4 Real Flight Data : QSSM

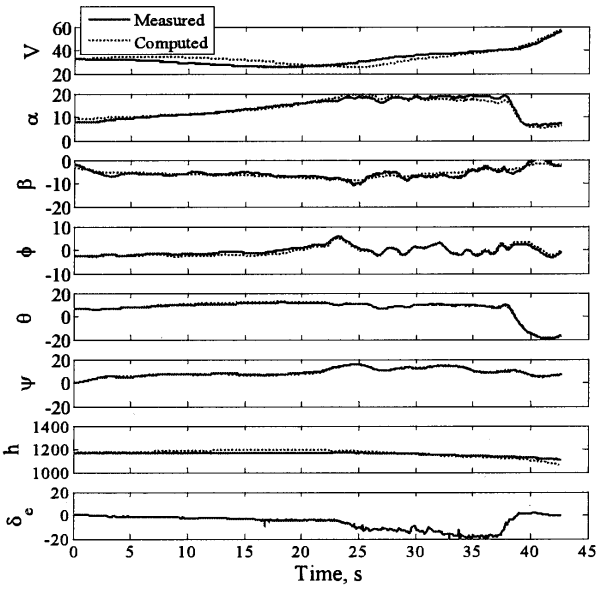

Fig.5 Data Compatibility Check : QSSM

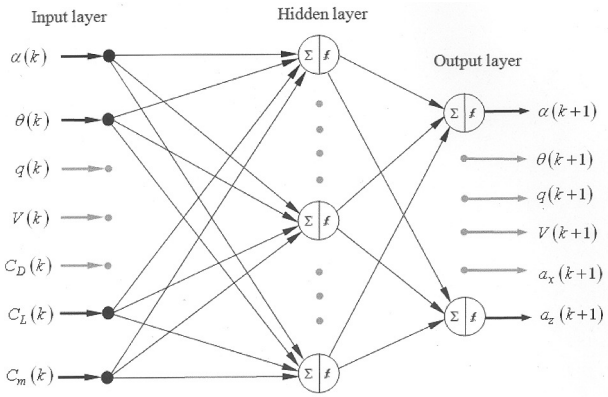

Fig.6 Neural-architecture for Longitudinal Flight Dynamic Model

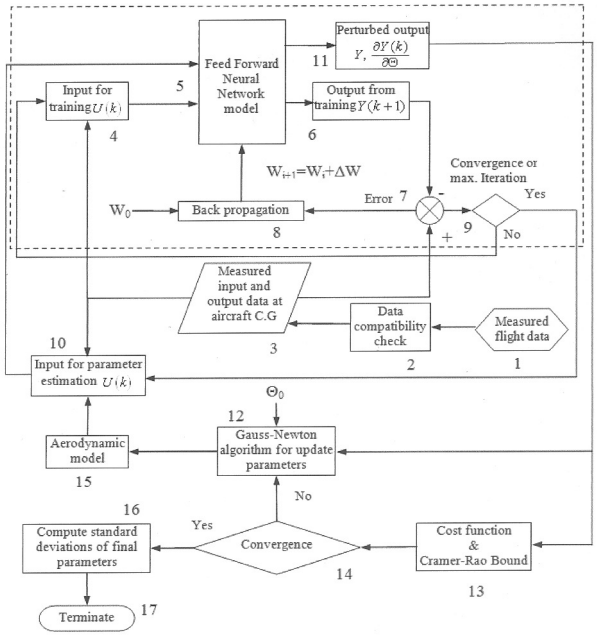

Fig.7 Schematic of NGN Method

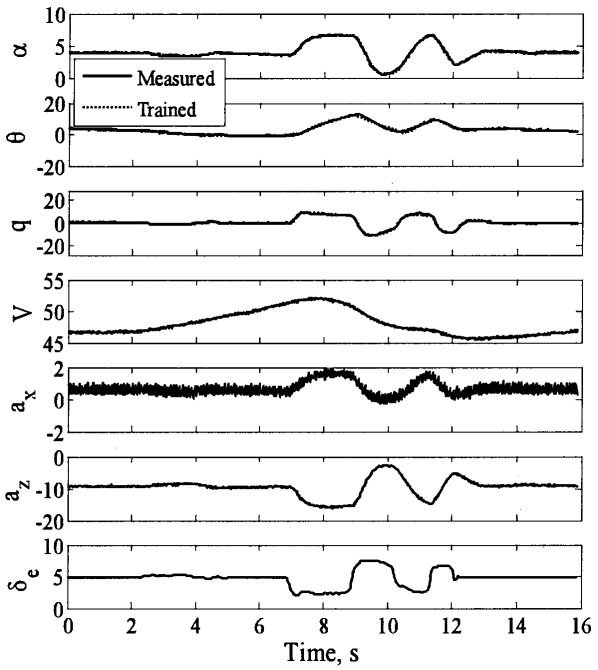

Fig.8 Measured and Trained Response Using NGN Method : 3-2-1-1 Input

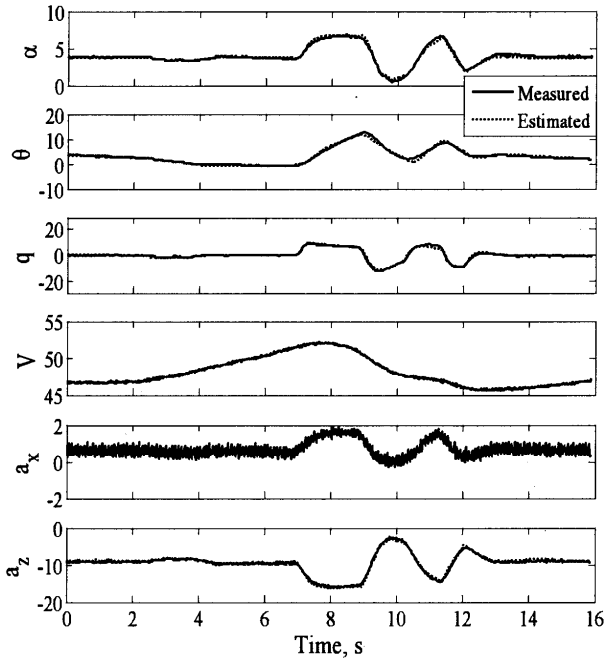

Fig.9 Measured and Estimated Response Using NGN Method : 3-2-1-1 Input

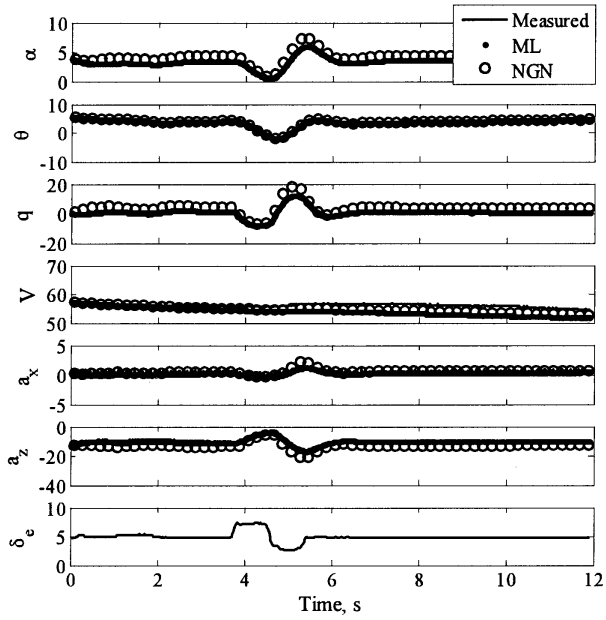

Fig.10 Parameter Estimation from 3-2-1-1 and Validation Using Doublet Input

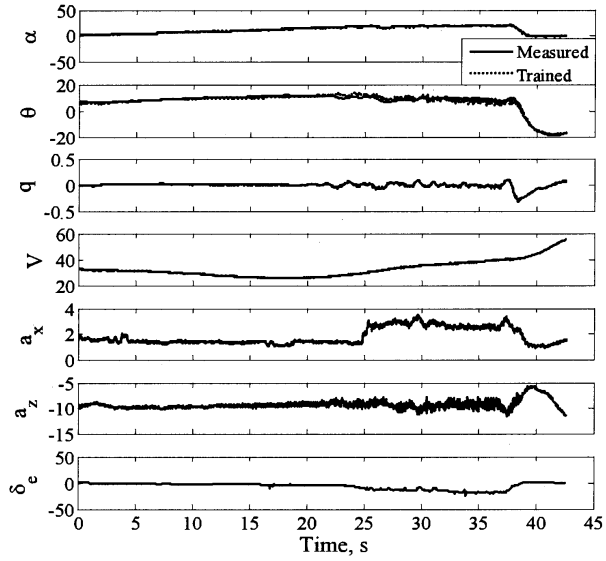

Fig.11 Measured and Trained Response Using NGN Method : QSSM

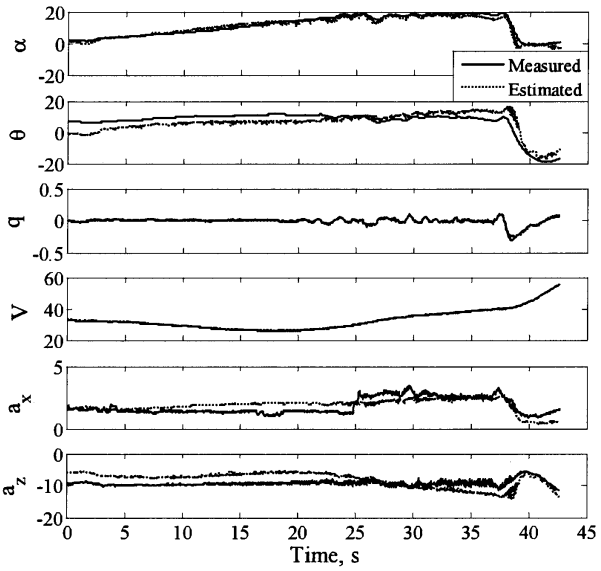

Fig.12 Measured and Estimated Response Using NGN Method : QSSM